# Laser-Induced Graphitization on a Diamond (111) Surface

C. Z. Wang,[1] K. M. Ho,[1] M. D. Shirk,[2] and P. A. Molian[2]

[1]*Ames Laboratory and Department of Physics and Astronomy, Iowa State University, Ames, Iowa 50011*

[2]*Department of Mechanical Engineering, Iowa State University, Ames, Iowa 50011*

(Received 5 April 1999)

We report an atomistic simulation study of laser-induced graphitization on the diamond (111) surface. Our simulation results show that the diamond to graphite transition occurs along different pathways depending on the length of the laser pulse being used. Under nanosecond or longer laser pulses, graphitization propagates vertically into bulk layers, leading to the formation of diamond-graphite interfaces after the laser treatment. By contrast, with femtosecond (0.2–0.5 ps) laser pulses, graphitization of the surface occurs layer by layer, resulting in a clean diamond surface after the ablation. This atomistic picture provides an explanation of recent experimental observations.

PACS numbers: 61.80.Ba, 68.35.Bs, 81.40.Wx

The behavior of semiconductor surfaces under intense laser-pulse irradiation is a subject of fundamental as well as technological interest. It has been observed that the structure and dynamics of the surface under laser-pulse irradiation are strongly dependent on the length of laser pulse being used [1–10]. Under nanosecond or longer laser-pulse irradiation, excited electrons can reach thermal equilibrium with the lattice within the duration of the laser pulse, leading to ordinary thermal disordering or melting on the surface. However, as the duration of the laser pulse is shortened to a femtosecond (0.2–0.5 ps) time scale, structural transformations on the surface can occur within a few hundred femtoseconds, which is much shorter than the typical time scale of lattice dynamics. This unusual structural transformation is believed to be driven by hot electron plasma excited by the intense femtosecond-laser pulse [11–13].

In this paper, we present an atomistic simulation of graphitization of the diamond (111) surface under nanosecond and femtosecond laser-pulse irradiation. Laser processing of bulk diamond and diamond thin films plays an important role in the microelectronics and cutting tool industries because the manufacture of diamond surfaces with low surface roughness and complex shapes has proven to be very difficult without laser ablation. Knowledge about laser-induced structural changes on the diamond surface at an atomistic level is useful not only for a better control of the quality of the laser-treated surface but also for a better understanding of the fundamental issues of laser irradiation. Our simulation results reveal different graphitization processes on the diamond (111) surface under two different regimes of laser ablation. The atomistic picture from our simulation provides an explanation of recent experiments on laser ablation of diamond surfaces.

In our simulations, interatomic interactions are described by an environment-dependent tight-binding carbon potential developed by Tang, Wang, Chan, and Ho [14]. This potential provides an accurate representation of the electronic band structures, cohesive energies, elastic constants, and phonon frequencies of crystalline carbon polytypes. It also predicts correctly the $\pi$-bonded chain $(2 \times 1)$ reconstruction for the diamond (111) surface. The reconstruction energy is found to be 0.65 eV per $(1 \times 1)$ surface unit cell which is in very good agreement with the *ab initio* calculation result of 0.68 eV [15]. The surface electronic states of the $(2 \times 1)$ reconstruction is also well described by the tight-binding potential. Explicit inclusion of the electronic structure in the tight-binding description allows us to investigate the behavior of the surface when the electrons in the system are highly excited. The accuracy and the quantum mechanical nature of the tight-binding potential makes the atomistic simulation of laser-induced structural change on the diamond (111) surface feasible.

For nanosecond or longer laser pulses, the excited electrons can transfer their kinetic energy to the lattice and reach thermal equilibrium with the lattice during the irradiation process, since the electron-lattice relaxation time is about $10^{-12}$ s [16]. Therefore, we can simulate the effect of nanosecond laser pulses by keeping the electrons and the lattice at the same temperature. In the case of femtosecond laser pulses, the laser energy is transferred to the electrons in a short time interval of only a few hundred femtoseconds which is much shorter than the electron-lattice relaxation time; thus, the energy deposited from the laser pulse will remain in the electron system and the lattice is not thermally equilibrated with the electrons. However, the duration of the laser pulse is longer than the relaxation time of the electron gas, which is about $10^{-14}$ s [16,17]. Therefore, we expect the electron system to be in thermal equilibrium at a high temperature while the lattice is cool under femtosecond laser irradiation.

Based on the above considerations, we have designed a tight-binding molecular dynamics scheme in which the occupation of electronic states in the system is described by a Fermi-Dirac distribution corresponding to a finite electron temperature $T_{el}$. Two sets of simulations are performed. In the first set of simulations, the electron temperature is equal to the lattice temperature to simulate a thermal process on the surface induced by nanosecond laser pulses. In

 0031-9007/00/85(19)/4092(4)$15.00 

another set of simulations to study the femtosecond irradiation, the electron system is set to a very high temperature while the lattice is allowed to evolve freely, with an initial temperature of 0 K.

The initial geometry is a 12-layer slab with 24 atoms per layer arranging in the $(2 \times 1)$ $\pi$-bonded chain reconstructed structure. Periodic boundary conditions are applied in the directions parallel to the surface. The forces governing the motion of the carbon atoms are derived from the Mermin free energy [18]

$$G = E + K_I - T_{\mathrm{el}} S_{\mathrm{el}}\,, \tag{1}$$

which includes the contributions from the electronic entropy

$$S_{\mathrm{el}} = -2k_B \sum_i [f_i \ln f_i + (1 - f_i)\ln(1 - f_i)] \tag{2}$$

as well as the tight-binding potential energy

$$E = 2\sum_i \varepsilon_i f_i + E_{\mathrm{rep}}\,, \tag{3}$$

where

$$f_i = \frac{1}{e^{(\varepsilon_i - \mu)/k_B T_{\mathrm{el}}} + 1} \tag{4}$$

is the Fermi-Dirac distribution function and $\mu$, the chemical potential, is adjusted every molecular dynamics (MD) step to guarantee the conservation of the total number of electrons:

$$2\sum_i f_i = N_{\mathrm{el}}\,. \tag{5}$$

$K_I$ in Eq. (1) is the kinetic energy of the atoms.

The simulations of thermal graphitization are performed at temperatures of 1500, 2000, 2500, and 2700 K. While the electron temperatures are fixed at desired values, the atomic temperatures are controlled by the velocity scaling method. The simulation results show that the $(2 \times 1)$ reconstruction structure is stable at temperatures below 2500 K during our simulation time of 10 ps. Graphitization of the diamond (111) surface proceeds rapidly when the simulation temperature reaches 2700 K. In Fig. 1, several instantaneous atomistic configurations from the simulation at the temperature of 2700 K are presented. It is interesting to note that the graphitization does not occur in a layer-by-layer fashion. Instead, graphitization occurs vertically; i.e., graphitelike regions penetrate into the bulk with the formation of diamond-graphite interfaces perpendicular to the surface. This phenomenon has also been observed in the previous *ab initio* MD simulation study of De Vita *et al.* [19].

The simulations of femtosecond laser ablation are performed with electron temperatures of 10 000, 13 000, 15 000 K, and higher. The atoms in the simulation are allowed to evolve freely while the electron temperature is kept at a constant value. At the electron temperature of 13 000 K or below, the diamond surface is retained within the simulation time of 500 fs. However, when the electron temperature reaches 15 000 K, a graphite layer peels off from the diamond surface within 300 fs of simulation time as one can see from Fig. 2(c). As the simulation is continued with a constant electron temperature of 15 000 K, the slab transforms into graphite sheets completely in 500 fs, in a layer-by-layer fashion. The layer-by-layer graphitization pathway is also found in all other higher electron temperature simulations, although the transition time becomes shorter when the electron temperature gets higher. At an electron temperature of 35 000 K, complete graphitization of the whole slab takes only about 100 fs.

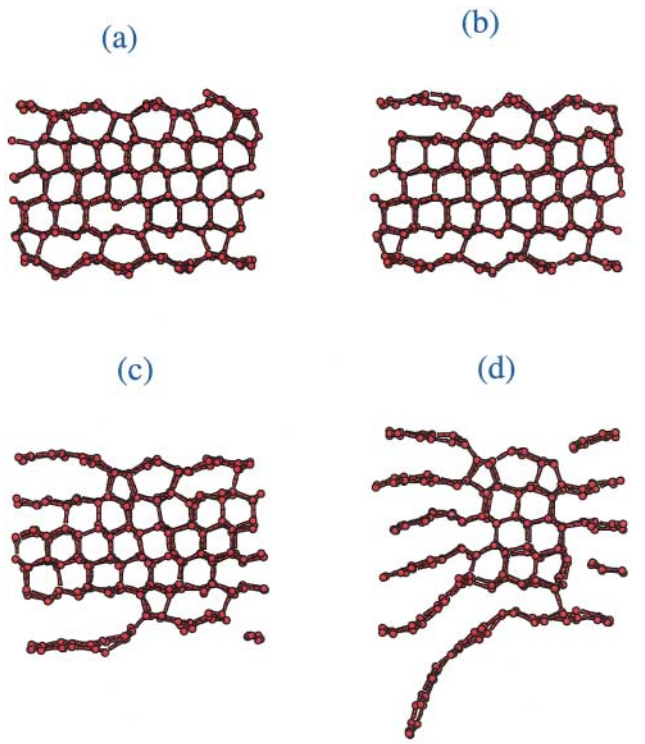


FIG. 1 (color). Graphitization of the diamond (111) surface via the thermal process. The snapshot pictures are taken at (a) 0 ps, (b) 1.0 ps, (c) 1.5 ps, and (d) 2.0 ps. The simulation is performed with the electrons and the atoms in thermal equilibrium at 2700 K. The plots show the side view of the simulation unit cell which is a 12-layer slab with two (111) surfaces (the top and bottom layers). Periodic boundary conditions are imposed in the plane parallel to the surface. Graphitization is found to occur through the formation of graphite-diamond interfaces [see (d)].

It was observed in experiments that diamond surfaces undergo structural changes after a nanosecond laser-pulse treatment, indicated by the loss of the characteristic Raman peak of diamond at 1332 $\mathrm{cm}^{-1}$ [1,2]. However, recent experiments by Shirk and Molian have shown that the 1332 $\mathrm{cm}^{-1}$ Raman peak is retained under intense ultrashort (200–500 fs) pulsed laser ablation [3]. The mechanism underlying the difference between the two types of experimental results was not well understood.

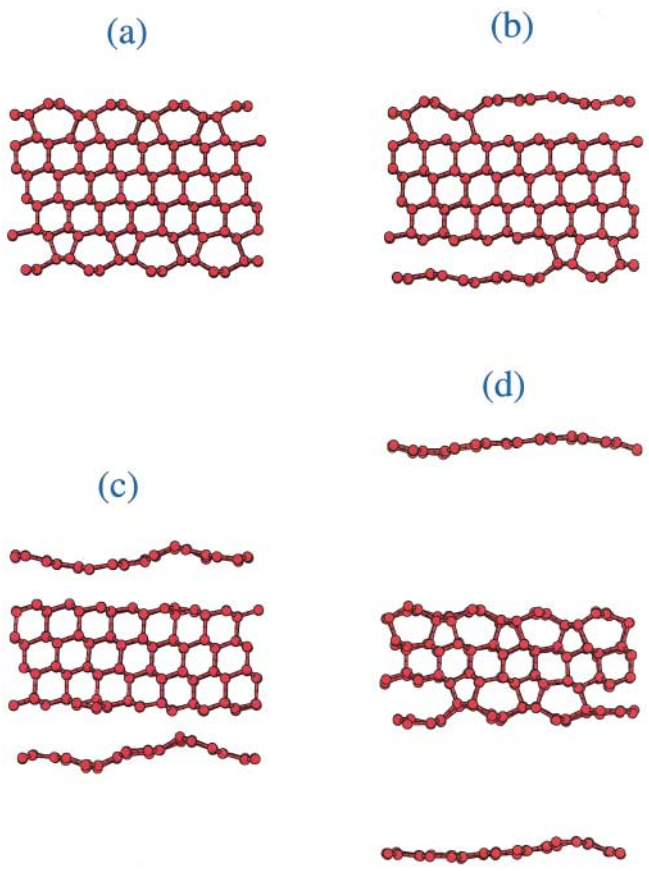


FIG. 2 (color). Graphitization of the diamond (111) surface due to the effects of hot electron plasma. The snapshot pictures are taken at (a) 0 fs, (b) 200 fs, and (c) 300 fs of simulation with an electron temperature of 15 000 K. (d) The result when the electron temperature is reduced gradually to room temperature after 300 fs of simulation at an electron temperature of 15 000 K. The orientation of the simulation unit cell is the same as specified in Fig. 1.

In our simulations discussed above, we established that the graphitization of the diamond (111) surface occurs along different pathways under long and short laser pulses. Because our simulations are performed at constant temperatures and with a very thin slab, continuous energy supply from the atomic and electronic heat baths will eventually turn the whole slab into graphite sheets. In the experiment, however, the graphitization has to stop at a certain point because the sample will cool down after the laser pulses. Our simulations suggest that the vertical graphitization process under the nanosecond laser pulses will lead to formation of vertical diamond-graphite interfaces when the sample is cooled down. This interface structure will remain on the surface after the laser pulses, leading to the loss of the 1332 $cm^{-1}$ Raman peak. On the other hand, since the femtosecond laser pulses peel off the carbon atoms from the surface layer by layer through a "nonthermal" mechanism, it will leave a smooth diamond surface.

In order to further verify the above conclusions, we repeated the simulations with a slightly different procedure. In the simulation of the thermal process, we cool down the system gradually after 2 ps of constant temperature simulation at 2700 K. The simulation results show that the graphite-diamond interface structure is, indeed, retained after the sample is cooled. In the simulations of the nonthermal process (i.e., ablation with femtosecond laser pulses), we allow the electron temperature to cool down to room temperature from its initial value of 15 000 K after 300 fs of simulation time. In that case, only one layer of graphite is observed to desorb from the diamond surface as one can see from Fig. 2(d).

An interesting question remains: Why does the graphitization by the thermal process take place in the vertical fashion rather than layer by layer? This phenomenon has also been observed by *ab initio* MD simulation [19], but no explanation has been given. We suggest that the different behavior can be understood in terms of the variation of the energy barrier for the diamond-to-graphite transition across the sample due to the presence of stress and a high lattice temperature. Because of the lattice mismatch between diamond and graphite, a tensile stress is created in the surface layer when part of it transforms into graphite. The lattice that is under the transformed region will be under compressive stress in the direction parallel to the surface. The difference in the in-plane thermal expansion of diamond and graphite makes this effect even more pronounced at high lattice temperatures [20]. If the energy barrier of graphitization decreases upon lattice contraction and increases upon lattice expansion, part of the lattice that is under compression will turn into graphite earlier than another part of the lattice which is under expansion. This will result in the formation of vertical diamond-graphite interfaces as observed in the simulation.

In order to verify our conjecture, we calculated the energy barrier of the diamond-to-graphite transition at zero lattice temperature following the rhombohedral transition pathway suggested previously [21,22]. For a given electron temperature, the total free energy (potential energy plus the contribution from the electronic entropy) of the system is a function of the intralayer and interlayer lattice constants of the rhombohedral lattice, and the interatomic distance of the two atoms in the rhombohedral unit cell. For a given intralayer lattice constant and a given interlayer distance, we find the free-energy minimum by varying the interatomic distance of the two atoms in the unit cell (in steps of 0.05 Å). In Fig. 3, these minimum energies as a function of interlayer distance are plotted for three given intralayer distances corresponding to the lattice constants of 3.50, 3.58, and 3.66 Å of diamond structure. Figure 3(a) shows the results at an electronic temperature of 2700 K, while Fig. 3(b) shows the results at an electronic temperature of 15 000 K. From the plots of Fig. 3, we can estimate the energy barrier as a function of the lattice constant of the diamond structure. These results, as

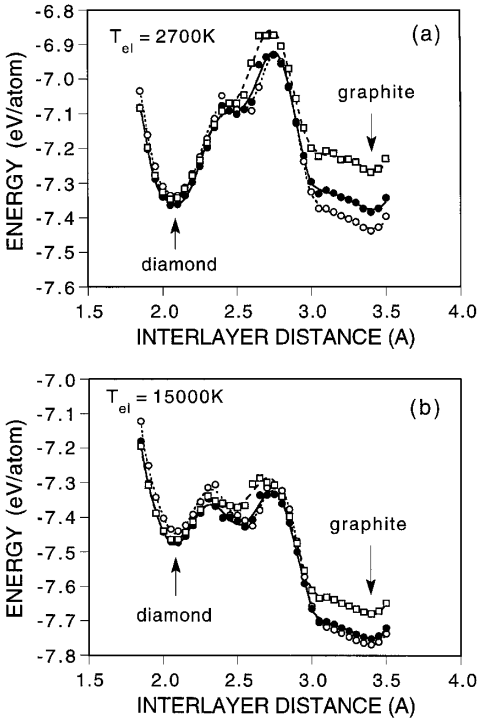


FIG. 3. The free energy (potential energy plus the contribution of electronic entropy) as a function of interlayer distance along the diamond to rhombohedral graphite transition path at three given intralayer lattice constants. (a),(b) The results at electron temperatures of 2700 and 15 000 K, respectively. The intralayer lattice constants correspond to the lattice constants of diamond structure at 3.50 Å (open circles and dotted lines), 3.58 Å (filled circles and solid lines), and 3.66 Å (open squares and dashed lines), respectively.

plotted in Fig. 4, clearly show that the energy barrier, indeed, increases as the lattice expands.

We also note that the energy barrier at the higher electron temperature of 15 000 K is much smaller than that at low electronic temperatures. This will make the graphitization transition much easier at high electronic temperatures. Although the energy barrier also increases with lattice constant, the effects of stress are smaller since the lattice is initially very cool. It is also interesting to note that the free energy of the graphite phase is much lower than that of the diamond phase at the high electron temperature of 15 000 K (by about 0.3 eV/atom). The free energy gain due to the initial graphitization at high electron temperature will help the system go through the complete transition very quickly.

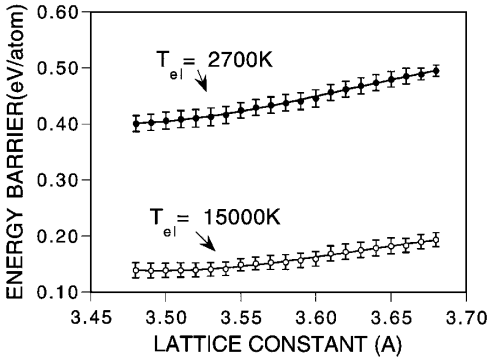


FIG. 4. Energy barriers for diamond to graphite transition as a function of diamond lattice constant. The filled circles are the results at an electron temperature of 2700 K. The open circles are the results at an electron temperature of 15 000 K. The equilibrium lattice constant of diamond at $T = 0$ from the present tight-binding potential is 3.585 Å.

The authors are grateful to Dr. James Morris for valuable discussions. This work was supported by the Office of Basic Energy Sciences, the High Performance Computing and Communications initiative (including a grant of computer time at the National Energy Research Supercomputing Center), the Ames Laboratory operated for the U.S. Department of Energy by Iowa State University, and the National Science Foundation.

[1] S. M. Pimenov, A. A. Smolin, V. G. Ralchenko, and V. I. Konov, Diam. Films Technol. **5**, 141 (1994).
[2] R. Windholz and P. A. Molian, J. Mater. Sci. **32**, 4295 (1997).
[3] M. D. Shirk and P. A. Molian, J. Laser Appl. **10**, 64 (1998).
[4] C. V. Shank, R. Yen, and C. Hirlimann, Phys. Rev. Lett. **50**, 454 (1983).
[5] C. V. Shank, R. Yen, and C. Hirlimann, Phys. Rev. Lett. **51**, 900 (1983).
[6] H. W. K. Tom, G. D. Aumiller, and C. H. Brito-Cruz, Phys. Rev. Lett. **60**, 1438 (1988).
[7] P. Saeta, J.-K. Wang, Y. Siegal, N. Bloembergen, and E. Mazur, Phys. Rev. Lett. **67**, 1023 (1991).
[8] S. V. Govorkov, T. Schroder, I. L. Shumay, and P. Heist, Phys. Rev. B **46**, 6864 (1992).
[9] K. Sokolowski-Tinten, J. Bialkowski, and D. von der Linde, Phys. Rev. B **51**, 14 186 (1995).
[10] I. L. Shumay and U. Hofer, Phys. Rev. B **53**, 15 878 (1996).
[11] J. A. Van Vechten, R. Tsu, F. W. Saris, and D. Hoonhout, Phys. Lett. **74A**, 417 (1979).
[12] P. Stampfli and K. H. Bennemann, Phys. Rev. B **42**, 7163 (1990).
[13] Note that we use the term "femtosecond," as do most other authors, even if "picosecond" is also appropriate.
[14] M. S. Tang, C. Z. Wang, C. T. Chan, and K. M. Ho, Phys. Rev. B **53**, 979 (1996).
[15] S. Iarlori, G. Galli, F. Gygi, M. Parrinello, and E. Tosatti, Phys. Rev. Lett. **69**, 2947 (1992).
[16] D. Agassi, J. Appl. Phys. **55**, 4376 (1984).
[17] E. J. Yoffa, Phys. Rev. B **21**, 2415 (1980).
[18] N. D. Mermin, Phys. Rev. **137**, A1441 (1965).
[19] A. De Vita, G. Galli, A. Canning, and R. Car, Nature (London) **379**, 523 (1996).
[20] B. Yates, *Thermal Expansion* (Plenum Press, New York and London, 1972), p. 69; A. C. Bailey and B. Yates, J. Appl. Phys. **41**, 5088 (1970).
[21] M. Kertesz and R. Hoffmann, J. Solid State Chem. **54**, 313 (1984).
[22] S. Fahy, S. G. Louie, and M. L. Cohen, Phys. Rev. B **34**, 1191 (1986).